

# Stoichiometry-Dependent Chemical Activity of Supported MgO(100) Films

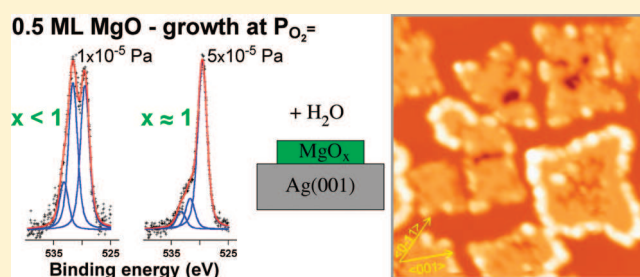
G. Cabailh,<sup>†</sup> R. Lazzari,<sup>†</sup> H. Cruguel,<sup>†</sup> J. Jupille,<sup>†</sup> L. Savio,<sup>‡</sup> M. Smerieri,<sup>‡,§</sup> A. Orzelli,<sup>§</sup> L. Vattuone,<sup>‡,§</sup> and M. Rocca<sup>\*,‡,§</sup>

<sup>†</sup>Institut des Nanosciences de Paris, CNRS and UPMC, 4 Place Jussieu, F75252 Paris, France

<sup>‡</sup>IMEM-CNR, Via Dodecaneso 33, 16146 Genova, Italy

<sup>§</sup>Dipartimento di Fisica, Università di Genova, Via Dodecaneso 33, 16146 Genova, Italy

**ABSTRACT:** Here, we show that the stoichiometry and, consequently, the chemical activity toward hydroxylation of MgO(100) films grown by reactive deposition on Ag(100) strongly depend on the O<sub>2</sub> partial pressure during film growth. Oxygen-deficient films undergo dramatic relative oxygen uptake either by exposure to a partial pressure of water vapor or by aging in vacuum for a sufficiently long time. Conversely, on stoichiometric monolayer MgO islands, photoemission analysis of the O 1s level and scanning tunneling microscopy images are consistent with the prediction that dissociative adsorption of water occurs only at the borders of the islands.



## 1. INTRODUCTION

The ubiquity of the interface between water and oxide materials, either in nature or in an industrial environment, has prompted a tremendous activity to determine the adsorption mechanisms at the microscopic scale on crystalline surfaces of simple oxides.<sup>1,2</sup> Among these, MgO offers the advantage of having various morphologies of good crystalline quality that involve cleaved crystal surfaces, high surface area samples, and supported films, all of these dominated by the low index (100) orientation.<sup>3,4</sup> On bulk MgO, the five-fold coordinated atoms of the basal (100) surface do not dissociate isolated water molecules in ultrahigh vacuum (UHV) conditions.<sup>5,6</sup> Adsorption was, however, reported for 12 monolayer (ML) thick films above 10<sup>-4</sup> mbar.<sup>7</sup> Conversely, water is easily dissociated at low-coordinated sites such as steps and kinks,<sup>1,2</sup> where they are predicted to give rise to many hydroxyl surface conformations.<sup>8</sup> For example, the same vibrational signature was found upon dissociative water adsorption on MgO smoke crystallites<sup>8</sup> and on multilayered MgO(100)/Ag(100) films<sup>4</sup> and ascribed to OH at monatomic <100> steps.

A puzzling case is the adsorption of water on supported MgO films in the submonolayer regime.<sup>9–14</sup> Three atomic plane thick MgO(100) films already show the electronic structure, band gap width, and reactivity of the bulk oxide surfaces of similar orientation.<sup>15</sup> Metal-supported MgO(100) films in the submonolayer range behave in a very different way. Upon exposure of those films to water vapor, the total coverage of additional hydroxyl groups has been estimated to be between 60 and 70% of a ML via the study of the area under the O 1s spectra.<sup>9,12,13</sup> Such an unexpected uptake has been attributed by Altieri et al.<sup>10</sup> to the peculiarities of the electronic properties of thin MgO(100) films supported on silver. These authors have suggested that

oxygen states in the vicinity of the Fermi level can hybridize and lower the activation energy for surface chemistry and that image charge screening both reduces the ionization potential and increases the affinity energy. On the contrary, Savio et al. ascribe the reactivity to the borders of the islands. Because the uptake at a given exposure decreases abruptly beyond monolayer MgO coverage, the high coverage is due to migration of the hydroxyls to their interior.<sup>12</sup> The observation of an enhanced reactivity of supported MgO films in the submonolayer range receives little support from numerical simulations. Density functional theory (DFT) hardly predicts any effect of the contact with the metallic support on both the electronic structure of MgO(100) and on its capacity to dissociate water.<sup>16</sup> Perfect MgO(100) islands are only expected to dissociate water molecules along their borders, no matter whether their orientation is polar or nonpolar.<sup>14</sup>

The existing data on the reactive behavior of silver-supported MgO films and the proposed interpretations are in conflict also for what concerns aging effects. After the exposure of freshly prepared MgO films in the submonolayer range to the residual atmosphere of the vacuum chamber for a few hours, Altieri et al.<sup>9,13</sup> observed the formation of an O 1s satellite peak of intensity similar to that observed by exposure to water vapor. Such a feature was attributed to OH contamination resulting from the water partial pressure in the residual gas, with a coverage on the order of a full monolayer.<sup>9,13</sup> However, performing similar

**Special Issue:** J. Peter Toennies Festschrift

**Received:** January 4, 2011

**Revised:** March 21, 2011

**Published:** April 29, 2011

experiments on MgO films of 1 ML or more, Savio et al.<sup>11,12</sup> found a more modest effect and, therefore, cast doubt on OH being the cause of aging.<sup>12</sup>

Those discrepancies might come from the composition of the islands. In particular, in the monolayer range, the stoichiometry of MgO films shows an extreme sensitivity to the conditions of synthesis, as demonstrated by high-resolution electron energy loss (HREEL) spectroscopy,<sup>17</sup> X-ray photoelectron spectroscopy,<sup>17–19</sup> (XPS) spot profile analysis low-energy electron diffraction,<sup>18</sup> and ellipsometry.<sup>19</sup> The present work explores this hypothesis. MgO films of different average stoichiometry were grown on Ag(100) under controlled conditions prior to being exposed to water vapor and/or aged in the vacuum chamber. The films were observed by scanning tunneling microscopy (STM), and the water uptake was analyzed by XPS.

## 2. EXPERIMENTAL METHODS

Photoemission experiments were performed at the University Pierre et Marie Curie (Paris 6). STM measurements were collected both in Paris, at room temperature (RT), and at the Physics Department of the University of Genoa, at 77 K. The two sets of data are in perfect agreement according to STM analysis. We report here STM images recorded in Genoa due to the higher quality resulting from the better stability of the low-temperature instrument. MgO was deposited by reactive deposition. Such a method is widely employed<sup>9,12,13</sup> because it is proposed to produce stoichiometric MgO films, provided it is operated in appropriate conditions.<sup>17</sup>

The Paris UHV setup involves a preparation stage, a photoelectron spectrometer consisting of a Omicron EA125 analyzer with an X-ray source, and a variable-temperature scanning tunneling microscope. XPS measurements were collected at normal emission, using the Al K $\alpha$  excitation source and at a background pressure better than  $3 \times 10^{-8}$  Pa. Spectra were fitted using a sum of Voigt functions, keeping the peak widths constant. For each spectrum, the background was modeled with a Shirley plus polynomial curve and a least-squares method, was used to optimize the fits. The peak positions were calculated with respect to the Ag 3d<sub>5/2</sub> binding energy, fixed at 368.2 eV. STM measurements were carried out on Omicron VT-STM/AFM. The Ag(100) crystal was prepared by cycles of argon sputtering (1 keV, 30° angle) with the sample held at 610 K and annealing to 810 K in UHV under a residual pressure lower than  $5 \times 10^{-10}$  mbar. The crystallographic quality and the cleanliness of the surface were checked using STM, low-energy electron diffraction (LEED), and XPS. A very sharp  $1 \times 1$  LEED pattern was recorded, and STM measurements showed very large terraces, with step heights of  $2.2 \pm 0.2$  Å in agreement with the interlayer distance of 2.05 Å in the  $\langle 001 \rangle$  direction. The carbon coverage was lower than 1% of a monolayer, as estimated from the C 1s area. No other contaminants were observed prior to deposition. The MgO thin films were prepared by reactive deposition with the Ag crystal at  $(465 \pm 10)$  K. The Mg effusion cell temperature was regulated at around 593 K, giving a Mg flux of approximately  $1.2 \text{ \AA}/\text{min}^{-1}$ , as estimated from the quartz microbalance. Oxygen was provided by backfilling the chamber. Two different oxygen partial pressures were used,  $P_{\text{O}_2} = 1 \times 10^{-5}$  Pa to obtain oxygen-deficient films and  $P_{\text{O}_2} = 5 \times 10^{-5}$  Pa to grow stoichiometric films.<sup>17,18</sup> The exact average thickness of the MgO film was determined by means of the Mg 2s/Ag 4s ratio corrected by the appropriate values of the ionization cross sections. Notice that

the corresponding binding energies are close enough to avoid any analyzer transmission function correction. A monolayer of MgO (ML) corresponds to an atomic layer of (100) orientation in bulk MgO. After several pump–freeze cycles, millipure water was dosed in the analysis chamber through a leak valve at pressures ranging between  $1 \times 10^{-7}$  and  $5 \times 10^{-7}$  Pa. Aging measurements were performed in the analysis chamber with a base pressure lower than  $1 \times 10^{-8}$  Pa. The exposure is defined in terms of Langmuir ( $1 \text{ L} = 1.33 \times 10^{-4} \text{ Pa/s}$ ).

The Genoa apparatus consists of a preparation chamber equipped for sample cleaning and MgO film growth and an analysis chamber, hosting the low-temperature STM (Createc) operated with liquid N<sub>2</sub>. The use of cryogenic temperatures allows the sample to remain uncontaminated for several days and, therefore, accurate probing of different sample areas. The lateral size of STM images and the orientation of the surface were determined from atomically resolved measurements of the clean Ag(100) surface; similarly, heights were calibrated on monatomic Ag steps. STM images were recorded in constant current mode, with bias voltages of  $-3.5 \leq V \leq +3.5$  V and with tunnelling currents of  $0.2 \leq I \leq 2.0$  nA. The tip was a W wire of 0.2 mm diameter, chemically etched and annealed under UHV. The Ag(100) crystal was prepared by cycles of sputtering with 1.5 keV Ne<sup>+</sup> ions and annealing at 750 K until a sharp LEED pattern was observed. MgO was deposited by reactive deposition while keeping the substrate at  $(500 \pm 10)$  K. During Mg evaporation, oxygen was provided through a doser approached at 1.5 cm from the substrate; the background pressure was thus kept at  $2\text{--}3 \times 10^{-5}$  Pa, while the effective pressure on the sample was enhanced by a factor of  $\sim 3$ .<sup>20</sup> The applied O<sub>2</sub> pressure was chosen to be 1 order of magnitude higher than that in our previous work<sup>12</sup> to ensure better stoichiometry. The average thickness of the MgO film was determined a priori by a quartz microbalance (Mg flux of  $\approx 1.5 \text{ \AA}/\text{min}$ ) and a posteriori by statistical analysis of STM images. Bidistilled water was dosed at RT by backfilling the chamber. Immediately after preparation, the sample was cooled to  $T < 120$  K and introduced into the STM. We estimate that postadsorption of water during this operation (lasting  $\sim 10$  min) is negligible with respect to the minimum H<sub>2</sub>O dose.

## 3. RESULTS

**3.1. Synthesis and Stoichiometry of MgO Films.** MgO films of thickness ranging from 0.35 to 1.2 ML were prepared and investigated by STM. In Figure 1, we compare 0.35 and 0.7 ML thick films, grown in Genoa under very similar O<sub>2</sub> partial pressure conditions. At the lower MgO coverage (panel A), the surface is covered with small MgO islands of irregular shape, while the 0.7 ML film (panel B) consists of larger, better shaped islands with borders mainly aligned along the nonpolar  $\langle 100 \rangle$  directions.<sup>15</sup> These are consistent with the expected Mg(100)/Ag(100) cube-on-cube epitaxy.<sup>16,21</sup> Borders along the  $\langle 110 \rangle$  polar orientations<sup>22,23</sup> are present but are definitively less frequent than nonpolar ones. MgO islands shown in Figure 1 mostly involve a single atomic layer, in agreement with the expectation that the MgO films grow almost layer-by-layer.<sup>15,24</sup> The apparent height of the islands shows a strong bias dependence due to the insulating nature of the oxide. At low bias voltage, the islands of panel B show an internal structure of irregular shape, which becomes barely visible for  $|V| > 3.0$  V. Under these conditions, indeed, tunneling takes place from the

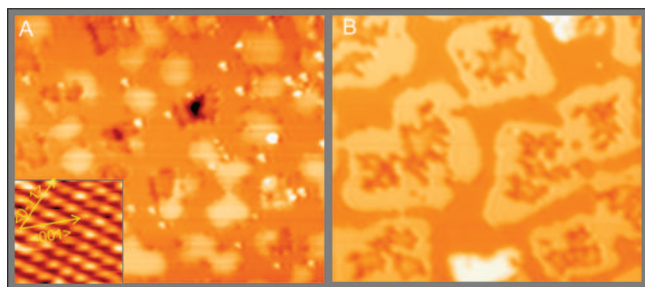


**Figure 1.** STM images recorded after deposition of MgO films of different thickness on Ag(100). (A) 0.35 ML MgO (image size: 33.0 nm  $\times$  28.4 nm,  $I = 0.44$  nA,  $V = 2.4$  V); (B) 0.7 ML MgO (image size: 33.0 nm  $\times$  28.4 nm,  $I = 0.36$  nA,  $V = 2.0$  V). Both films were grown by reactive deposition under  $O_2$  partial pressures of  $1.3 \times 10^{-3}$  and  $1.8 \times 10^{-3}$  Pa, respectively, given through a doser at 1.5 cm from the sample surface. The inset of panel A shows an atomically resolved image of the clean Ag(100) surface. High symmetry directions are also indicated.

conduction/valence band of MgO into the filled/empty states of the tip, and topographic imaging is achieved. The internal structure indicated thus has electronic rather than topographic nature. Although the dependence of the internal island morphology versus important growth parameters, such as stoichiometry and substrate temperature, during evaporation is still under investigation, we can state here that (1) because their apparent height is bias-dependent, the dark spots inside of the monolayer MgO islands do not correspond to “holes” in the islands revealing the Ag substrate underneath and (2) the presence of an internal structure of the islands is very common for the 0.7 ML film but much less frequent for the 0.35 ML one. On the other hand, it is not evident on multilayer films.<sup>4</sup> The observed behavior suggests that this structure is due to a particular arrangement of MgO units (possibly in nonstoichiometric conditions), that it develops with increasing coverage up to 1 ML, and that is no longer detectable if a second layer is present. As shown in the following, however, it is not a preferential site for water adsorption/dissociation at least for MgO islands close to stoichiometric composition.

The stoichiometry of MgO films has been determined by XPS from the ratio of the areas of the O 1s and Mg 2s core level peaks corrected by the ionization cross sections<sup>25</sup> and by the analyzer transmission function. The latter parameter was established experimentally from the ratio of spectra recorded in fixed retardation mode and the constant analyzer energy on polycrystalline stainless steel.<sup>26</sup> The negligible concentration of multilayer islands (see Figure 1) rules out possible photodiffraction effects. The so-determined stoichiometry is reported in Table 1 for films of different thickness and produced under different  $O_2$  partial pressure. For reasons that stem from both the uncertainty on the ionization cross sections and transmission function and the exact geometry of the supported film, the O 1s/Mg 2s area ratio cannot be taken as an absolute measurement of the MgO content. It is only indicative that layers prepared under  $P_{O_2} = 1 \times 10^{-5}$  Pa are oxygen-deficient while growth in  $P_{O_2} = 5 \times 10^{-5}$  Pa leads to a stoichiometry much closer to unity, in agreement with the observations of Pfnür et al.<sup>17,18</sup>

The O 1s spectra of the pristine MgO films are dominated by a component at binding energy  $E_b(O\ 1s) \approx 529.7$  eV, corresponding to O atoms of the MgO lattice. This is evident from the left panels of Figure 2, recorded on films 1, 2, and 3 of Table 1.

**Table 1.** Stoichiometry of the MgO Films under Study, As Estimated via the Ratio of the O 1s and Mg 2s Core Level Areas Measured by XPS (see text)

|            | oxygen partial pressure (Pa) | reference | stoichiometry O/Mg of the film | coverage in ML |
|------------|------------------------------|-----------|--------------------------------|----------------|
| monolayer  | $1 \times 10^{-5}$           | film 1    | 0.75                           | 0.39           |
|            | $5 \times 10^{-5}$           | film 2    | 1.03                           | 0.42           |
| multilayer | $1 \times 10^{-5}$           | film 3    | 0.88                           | 1.2            |

The origin of the satellites peaks at higher binding energy is discussed in the paragraph dedicated to water adsorption. The binding energy of the main O 1s line increases from 529.4 eV for a 0.5 ML film to 529.9 eV for a 3.0 ML film. In parallel, the Mg 1s core level shifts from 1302.9 to 1303.1 eV. For submonolayer MgO films,  $E_b(O\ 1s)$  was found at values ranging from 528.4<sup>13</sup> and 528.5<sup>17</sup> to 530.0<sup>17</sup> and 530.5 eV.<sup>12</sup> The former two references show also an  $E_b(O\ 1s)$  upshift with MgO coverage that is qualitatively similar but quantitatively larger (more than 2 eV) than that reported in the present paper, while Savio et al. found the same O 1s value at all MgO coverages. In parallel, shifts of 0.9<sup>27</sup> and 0.5 eV<sup>17</sup> of the Mg 1s line were observed. Moreover, by annealing at 400 and then at 800 K a 0.5 ML thick MgO film grown at 300 K, Peterka et al. have reported  $E_b(O\ 1s)$  shifts from 528.5, to 530.0, and to 530.9 eV,<sup>17</sup> a phenomenon assigned to changes in the structural and electronic configurations at the interface. Notably, the  $E_b(O\ 1s)$  values (529.4–529.9 eV) found in the present investigation for MgO films synthesized at 465 K and assumed to be close to stoichiometry are comparable to the value (530.0 eV) recorded by Peterka et al. for similar films synthesized at 400 K.<sup>17</sup> Generally speaking, the above results demonstrate that the binding energy of the O 1s level of MgO films supported on Ag(100) is extremely sensitive to the conditions of pressure and temperature in which the film is synthesized and to its aging (see below).

**3.2. Exposure to Water Vapor.** The sequences of XPS spectra shown in Figure 2 correspond to water uptake experiments performed on films 1 (panel A), 2 (panel B), and 3 (panel C) presented in Table 1. As already stated, the presence of the adsorbate is revealed by a significant increase of the O 1s satellite peak at 532 eV, while no modifications of the 534.2 eV feature and of the Mg 1s position (within 0.1 eV) and intensity (within 2%) were observed. Each O 1s spectrum was fitted with the sum of three Voigt functions having a Lorentzian width of 0.8 eV. The Gaussian width was constrained to be identical for all components for a given fit. For films 1 and 2, it was set at 1.6 eV and allowed to vary within  $\pm 0.1$  eV. For film 3, it was fixed at  $1.4 \pm 0.1$  eV. The O 1s satellite peaks are at  $(2.3 \pm 0.3)$  and  $(4.2 \pm 0.5)$  eV higher binding energies, respectively, with respect to the main O 1s level (Figure 2). They are already present in the O 1s spectra of the bare MgO films, and their evolution with water exposure is quite different for the three samples. About the decomposition of the O 1s spectra, it is important to notice that no series of O 1s spectra could be fitted just with two peaks while keeping one given Gaussian width for both peaks. Therefore, despite its weak intensity, the O 1s component at 534.2 eV corresponds to a real oxygen species.

The absolute and relative intensities, presented in Figure 3, allow a more quantitative discussion. Upon water adsorption, the increase in intensity of the 532 eV component dominates the change in the O 1s profile. This feature is assigned to OH formed by the heterolytic dissociation of water molecules on the MgO

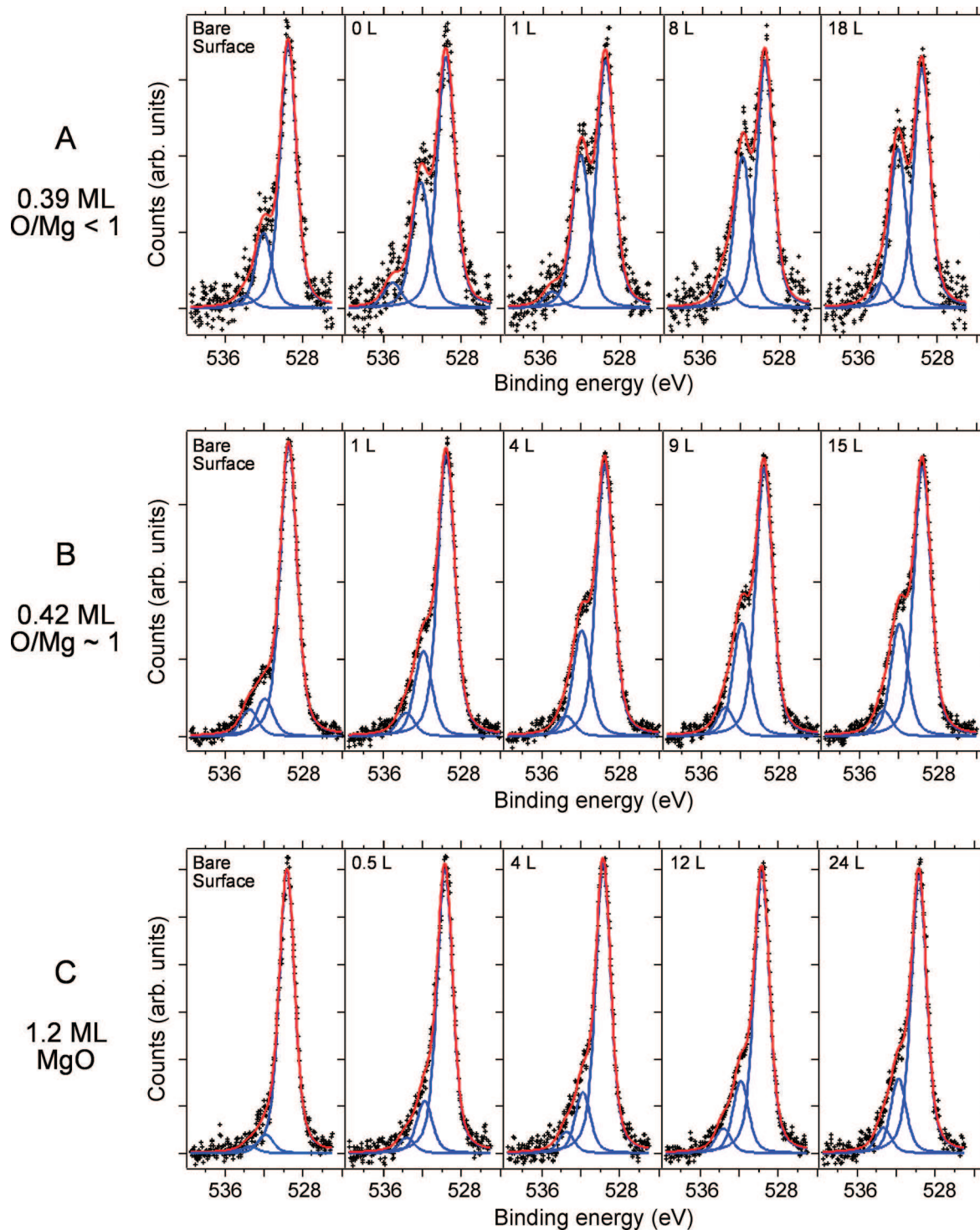


**Figure 2.** XPS spectra recorded during the exposure of (A) film 1 (0.39 ML thick film, oxygen-deficient, labeled O/Mg < 1), (B) film 2 (0.42 ML thick film, close to stoichiometry, labeled O/Mg  $\sim$  1), and (C) film 3 (MgO coverage > 1 ML) to water vapor at RT (films as defined in Table 1).

films, in accord with literature.<sup>4,9,12–14</sup> The existence of an intrinsic contribution appearing at a similar energy on the bare surface cannot be unambiguously proved because the delay between the preparation and the analysis of the film is sufficiently long to allow for a sizable adsorption from the residual gas. In particular, in Figure 2A, there is a difference between the spectrum of the bare surface of the oxygen-deficient MgO film

and the spectrum collected before dosing water (labeled 0 L in the figure). Such a difference corresponds to the exposure to the residual gas during the time needed to record various reference spectra (about 1 h). On the contrary, the relative intensity of the satellite at 534.2 eV hardly shows any variation during exposure (Figure 3), which discards any link with water uptake<sup>13</sup> and suggests the existence of an intrinsic chemistry of the MgO film

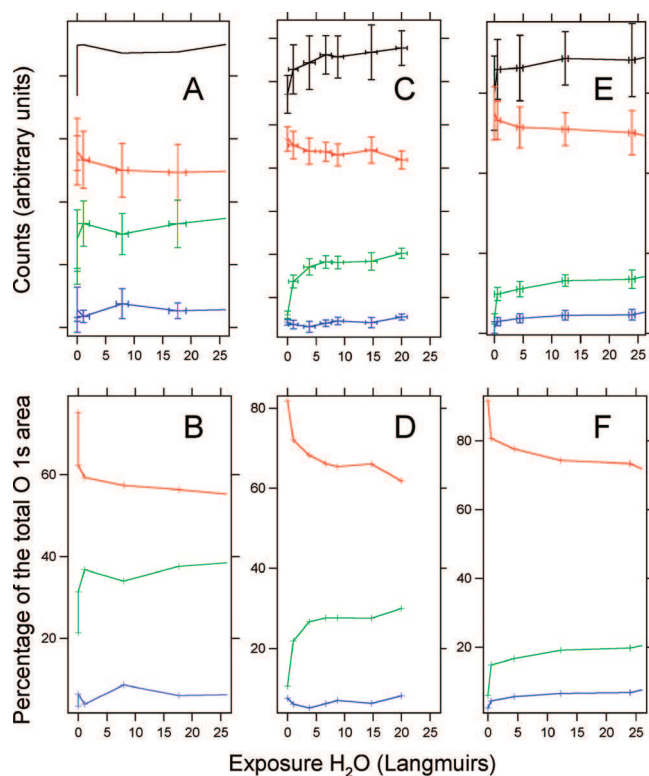


**Figure 3.** Evolution of the intensity of the O 1s components during exposure of MgO/Ag(100) to water vapor at RT: (A,B) film 1, (C,D) film 2, and (E,F) film 3 as defined in Table 1. (A,C,E) Absolute areas under the O 1s components corresponding to lattice oxygen (red), a  $2.3 \pm 0.3$  eV shift (green), a  $4.2 \pm 1.0$  eV shift (blue), and the overall O 1s area (black). (B,D,F) Relative areas with respect to the total O 1s area, with the same color code. The same vertical range was used for each set of experiments to allow an easier comparison.

with the formation of an extra oxygen species. Similar satellites shifted by 2–3 eV with respect to the main line were observed in the O 1s spectra of pristine MgO films grown on Mo(001)<sup>28</sup> and Ru(001).<sup>29</sup> In qualitative agreement with Peterka's hypothesis of the formation of MgO<sub>2</sub><sup>17</sup> and in line with the present assumption, they were assigned to either peroxide species<sup>28</sup> or dioxygen, or partially reduced oxygen species.<sup>29</sup>

Exposure of MgO films to water vapor results in the growth of the O 1s satellite peaks at higher binding energy (Figure 2). The three series of O 1s spectra, presented in Figure 2, show the same O 1s components but different intensities, which suggests the presence of identical species with different coverages. This is in particular true for the 532.0 eV satellite. Its absolute increase indicates that a net OH uptake is always present, leading to the formation of some Mg(OH)<sub>2</sub>, although in different amounts depending on the film conditions. Indeed, the 532 eV peak relative weight with respect to the whole O 1s area decreases in the order film 1 > film 2 > film 3. Relative values are 41, 29, and 21% (Figure 3, bottom), respectively, for the largest H<sub>2</sub>O exposure. The salient point raises from the comparison of films 1 and 2, which have very similar thicknesses (0.39 and 0.42 ML, respectively) but significantly different stoichiometries, having been grown under different O<sub>2</sub> partial pressures. The reactivity of the less stoichiometric film toward hydroxylation is increased with respect to the stoichiometric one, as demonstrated by the higher O 1s signal at 532 eV measured upon water exposure.

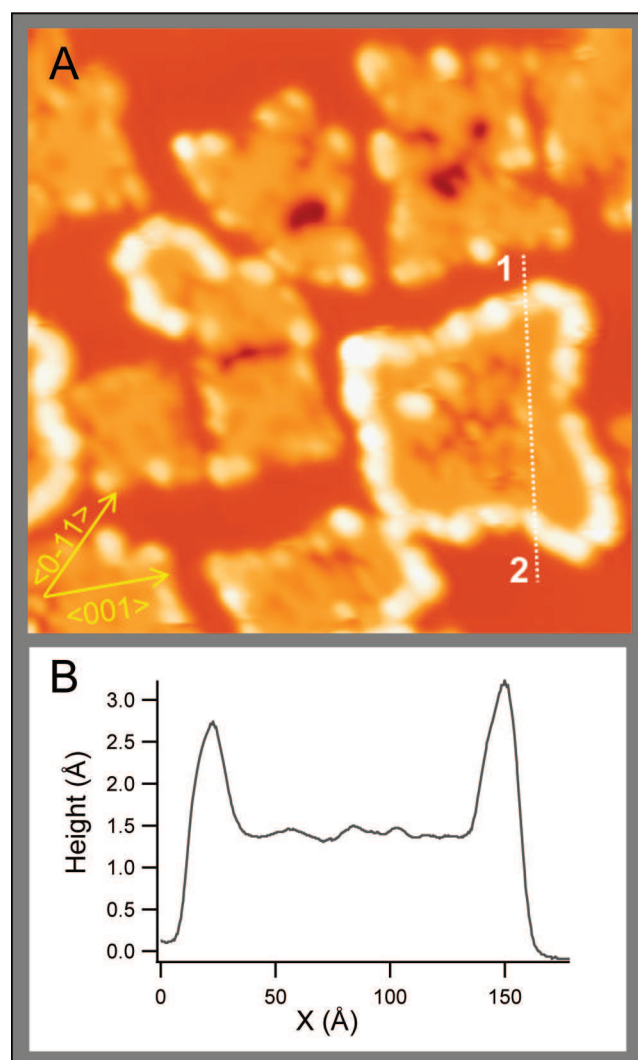


**Figure 4.** (A) STM image of a 0.7 ML MgO film after exposure to 2 L of water vapor at 300 K (see text). Hydroxyl groups are evident as bright features decorating the borders of the MgO islands. The high symmetry directions are marked (image size 33 nm × 33 nm,  $I = 0.43$  nA,  $V = 2.0$  V). (B) Height profile measured from point (1) to (2) along the dotted line in panel A and showing the apparent increase in height due to the OH groups with respect to the MgO island.

The reduced reactivity with respect to water of the 1.2 ML film is expected from previous spectroscopic data.<sup>12</sup>

In parallel, OH decoration of island borders is observed by STM. Films for STM analysis (Figures 1 and 4) were grown in an O<sub>2</sub> partial pressure comparable to that used to prepare film 2 and are therefore expected to show the same reactivity with respect to water vapor. Figure 4 reports a STM image recorded after exposing a 0.7 ML MgO film to 2 L of H<sub>2</sub>O at RT. The bright spots that decorate the island borders are attributed to adsorbed hydroxyl groups on the basis of previous HREELS results<sup>11,12</sup> and of the present XPS analysis. No traces of H<sub>2</sub>O/OH adsorption are detected away from the border of the islands, which maintain their internal structure. Therefore, at least in the limit of low exposures, dissociative adsorption at the low-coordinated sites of the MgO island borders is strongly favored. This result is in agreement with theoretical predictions.<sup>14</sup> Migration of OH units toward the MgO(100) terraces for higher OH

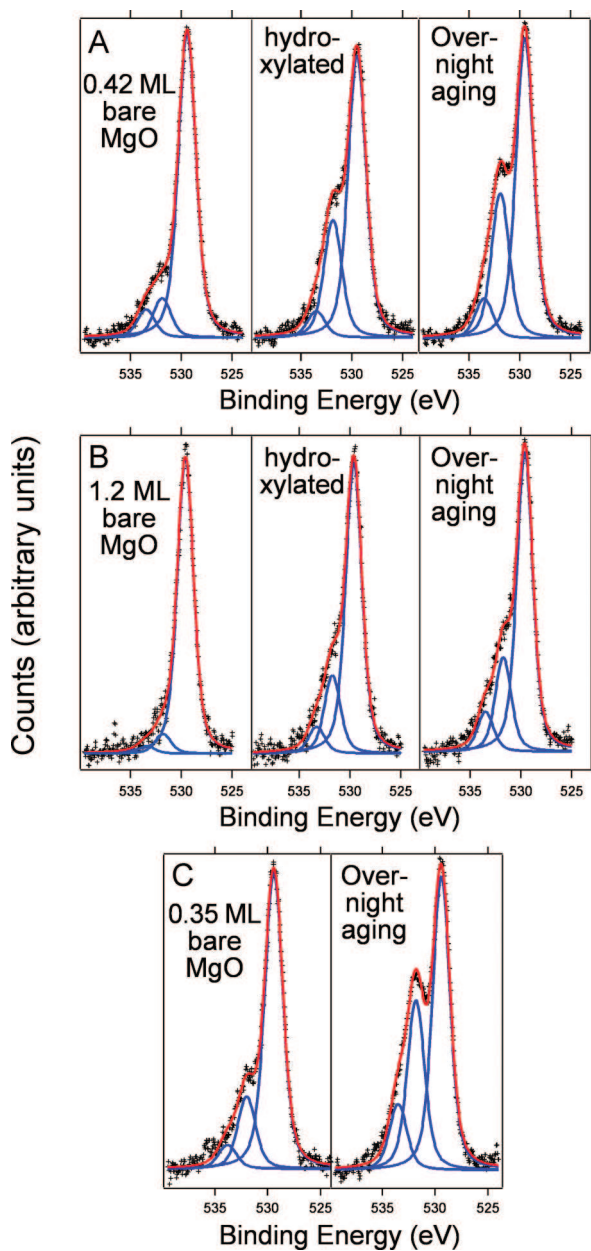


**Figure 5.** Aging of MgO films prepared: (A) under an oxygen pressure of  $5 \times 10^{-5}$  Pa and thus close to stoichiometry. Overnight aging (right spectrum) of film 2 of Table 1 after hydroxylation; spectra recorded on the bare surface (left spectrum) and on the fully hydroxylated surface (middle spectrum, already shown in Figure 2b, are reproduced). (B) Same as (A) regarding film 3 grown at  $1 \times 10^{-5}$  Pa. (C) overnight aging of a 0.35 ML thick film grown at  $5 \times 10^{-5}$  Pa without previous hydroxylation.

coverages<sup>11,12</sup> cannot be excluded but is unlikely. The few bright spots that appear close to the center of the islands may correspond to water molecules adsorbed at point defects.<sup>30</sup>

**3.3. Aging of the MgO Films in UHV.** Figure 5 reports XPS O 1s spectra recorded after aging in the residual atmosphere of the vacuum chamber of hydroxylated (panels A and B) and bare (panel C) films. The former correspond to overnight aging of films 2 and 3 (Table 1) previously hydroxylated close to saturation. The change due to aging is marginal. By comparison, the spectrum in Figure 5C was observed on a 0.35 ML thick film

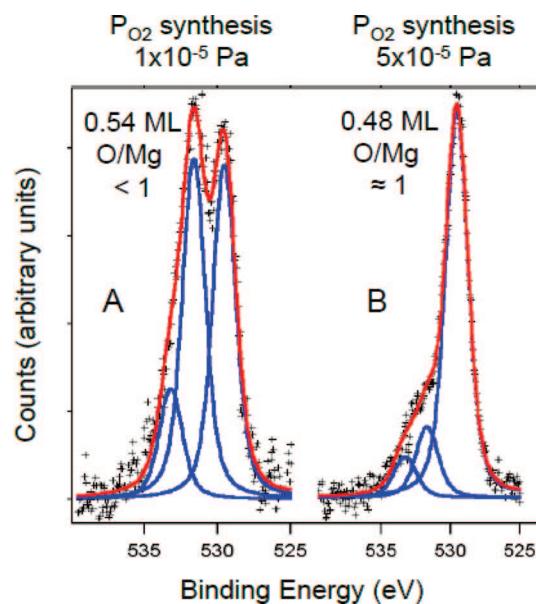


**Figure 6.** MgO films aged in vacuum: comparison between films prepared under (A)  $1 \times 10^{-5}$  Pa O<sub>2</sub> of oxygen (O/Mg < 1) and (B)  $5 \times 10^{-5}$  Pa O<sub>2</sub> (O/Mg  $\approx$  1). Note the very different intensity of the 2.3 eV satellite (see text). These films are among the samples dedicated to STM study that were only exposed to the residual atmosphere and analyzed by XPS after aging without recording the initial spectra.

prepared under  $5 \times 10^{-5}$  Pa of O<sub>2</sub> for which the O 1s/Mg 2s area ratio is 0.81. That film is very close to film 2 (Table 1), and its overnight aging leads to an O 1s spectrum comparable to that recorded on film 2 after hydroxylation and aging (Figure 5A). The carbon coverage was checked to remain marginal during the aging process, so that interactions with carbon monoxide or carbon dioxide were discarded. Such behavior proves that the oxygen uptake stems from adsorption of water from the residual atmosphere of the vacuum chamber. By fitting the spectra with three components, similar binding energies as those determined after exposure to water vapor (Figure 2) were found for aged films (i.e.,  $2.3 \pm 0.3$  and  $4.0 \pm 0.5$  eV, Figure 5C). On the basis of the O 1s binding energy, it is assumed that exposure to water vapor and aging in UHV of the MgO films result in a hydroxylation of the film via dissociative adsorption of water molecules. Moreover, both the small change observed by aging of hydroxylated surfaces (Figure 5A and B) and the similarity of the oxygen uptake upon either exposure to water vapor or aging (Figure 5C compared to Figure 5A) indicate that similar sites are populated in the two cases.

The trends described herein were quite systematically observed. Figure 6 shows two O 1s spectra recorded on half-monolayer MgO films, grown under  $1 \times 10^{-5}$  (Figure 6A) and  $5 \times 10^{-5}$  Pa (Figure 6B), respectively, and aged overnight. These films are representative of samples with different stoichiometries and show that, for a lattice oxygen deficient case (Figure 6A), aging can lead to an additional oxygen signal even larger than the lattice one. On the contrary, for the more stoichiometric case (Figure 6B), the overnight O addition is significantly lower.

The present conclusions apparently contradict those reported in a previous paper by Savio et al.<sup>12</sup> in which the aging phenomenon, analyzed for MgO films of 1 ML or more by XPS and HREELS, could not be correlated to an increase of the OH stretch signal; it was therefore suggested not to be due to

hydroxylation by the residual water vapor. However, the present work demonstrates that the reactivity of the MgO films depends critically not only on their thickness<sup>11</sup> but also on their stoichiometry and that it is in the submonolayer range (not explored in the work of Savio et al.) that strong effects can be observed. Therefore, the different chemical behavior reported in the literature can be rationalized by the different quality of films and rest gas obtained in different experimental runs. In this frame, the absence of correlation between the satellite peak at 532.6 eV and the OH stretch signal reported in ref 12 for 1 ML films can be explained by the good stoichiometry and, consequently, the low reactivity of the samples that we examined by HREELS.

#### 4. DISCUSSION

Strong oxygen uptakes by submonolayer MgO films,<sup>13</sup> such as those observed in Figures 2A and 6A, have been assigned to a particularly reactive behavior of the (100) terraces, which was suggested to mainly arise from specific hybridization and from image potential screening of charge fluctuations.<sup>9</sup> These views contradict the prediction by density functional approaches that, even in the monolayer range, stoichiometric MgO islands dissociate water molecules on their borders only.<sup>14</sup> It is shown herein that, when prepared under  $1 \times 10^{-5}$  Pa of oxygen (Figures 2A and 6A), MgO films in the monolayer range are clearly more reactive toward water vapor than films synthesized under  $5 \times 10^{-5}$  Pa of O<sub>2</sub> (Figures 2B, 5A and C, and 6B). This observation unambiguously links the O/Mg stoichiometry of the islands (Table 1) and the ability to apparently dissociate water on the (100) plane. Moreover, it demonstrates a posteriori the consistency of the use of the O 1s/Mg 2s ratio to define the MgO stoichiometry (section 3.1). Indeed, after aging of the stoichiometric film of 0.48 ML (Figure 6B), the relative intensity of the satellite at 2.3 eV reaches 15% of the lattice O 1s peak intensity. This is even smaller than that (20%) observed on the multilayered 1.2 ML film (film 4, Figures 2C and 4E and F), on which the hydroxylation is expected to occur only on step edges.<sup>9,12</sup> The relative area of 15% of the 2.3 eV satellite (Figure 6D) can be accounted for by a film consisting of  $6 \times 6$  nm<sup>2</sup> MgO square islands with fully hydroxylated nonpolar edges that are a reasonable representation of the MgO islands shown in Figures 1B and 4A, if taking geometric defects into account. Consistently, STM shows that after exposure to 2 L of water vapor, the borders of the islands involved in a 0.7 ML MgO film are nicely decorated by what is assigned to hydroxyl groups. Therefore, as expected from density functional theory,<sup>14</sup> XPS and STM data recorded on films close to stoichiometry are consistent with water dissociation at the island edges only, while perfect (100) MgO planes are inert in the limit of low water pressure and exposure.

Hydroxylation of MgO(100) terraces also occurs at high enough water vapor pressure.<sup>5,6</sup> Pressures at which water was dosed by Altieri et al. ( $5 \times 10^{-6}$  Pa),<sup>13</sup> Savio et al. ( $2 \times 10^{-6}$  Pa),<sup>12</sup> and in the present experiment ( $5 \times 10^{-7}$  Pa) range within 1 order of magnitude. This difference might play a role for the hydroxylation of the terraces because the threshold pressure for this process was reported to decrease with layer thickness and to be at  $10^{-6}$  Pa for the bilayer (see Figure 3 of ref 7). Nevertheless, the full hydroxylation of terraces is only observed at a water vapor pressure of  $\sim 1$  Pa, which is far beyond the pressure range under discussion herein. The present finding of an O 1s satellite shifted by 2.3 eV relative to the main line is in agreement with the values of 1.9<sup>31</sup> and 2.3 eV<sup>5</sup> found on bulk MgO crystals and of 2.1 eV

recorded on MgO/Ag(100) thin films.<sup>12</sup> The shift was attributed to OH groups either on the basis of its strong dissimilarity with the O 1s shift of 3.6 eV due to molecularly adsorbed water<sup>31</sup> or because it was observed in conditions that showed no scissor mode at 1660 cm<sup>-1</sup> by high-resolution electron energy loss spectroscopy.<sup>12</sup>

#### 5. CONCLUSION

Stoichiometric MgO films in the monolayer range were prepared by reactive deposition of magnesium in appropriate conditions (flux of 1 ML per minute on Ag(100) crystals at 460–470 K, under a partial pressure of oxygen of  $5 \times 10^{-5}$  Pa). As expected from density functional approaches, these films behave in the same way as the surface of bulk samples with respect to the adsorption of water. XPS and STM data are consistent with the prediction that water molecules only dissociate on the low-coordinated sites of the island edges and not on the (100) planes.

#### AUTHOR INFORMATION

##### Corresponding Author

\*E-mail: rocca@fisica.unige.it.

#### REFERENCES

- (1) Brown, G. E.; Heinrich, V. E.; Casey, W. H.; Clark, D. L.; Eggleston, C.; Felmy, A.; Goodman, D. W.; Gratzel, M.; Maciel, G.; McCarthy, M. I.; Nealon, K. H.; Sverjensky, D. A.; Toney, M. F.; Zachara, J. M. *Chem. Rev.* **1999**, *99*, 77.
- (2) Henderson, M. A. *Surf. Sci. Rep.* **2002**, *46*, 1.
- (3) Spoto, G.; Gribov, E. N.; Ricchiardi, G.; Damin, G.; Scarano, D.; Bordiga, S.; Lamberti, C.; Zecchina, A. *Prog. Surf. Sci.* **2004**, *76*, 71.
- (4) Savio, L.; Smerieri, M.; Orzelli, A.; Vattuone, L.; Rocca, M.; Finocchi, F.; Jupille, J. *Surf. Sci.* **2010**, *604*, 252.
- (5) Liu, P.; Kendelewicz, T.; Brown, G. E., Jr.; Parks, G. A. *Surf. Sci.* **1998**, *412–413*, 287.
- (6) Abriou, D.; Jupille, J. *Surf. Sci.* **1999**, *430*, L527.
- (7) Carrasco, E.; Brown, M. A.; Sterrer, M.; Freund, H.-J.; Kwapien, K.; Sierka, M.; Sauer, J. *J. Phys. Chem. C* **2010**, *114*, 18214.
- (8) Finocchi, F.; Hacquart, R.; Naud, C.; Jupille, J. *J. Phys. Chem. C* **2008**, *112*, 13226.
- (9) Altieri, S.; Tjeng, L. H.; Sawatzky, G. A. *Phys. Rev. B* **2000**, *61*, 16948.
- (10) Altieri, S.; Tjeng, L. H.; Sawatzky, G. A. *Thin Solid Films* **2001**, *400*, 9.
- (11) Savio, L.; Celasco, E.; Vattuone, L.; Rocca, M. *J. Chem. Phys.* **2003**, *119*, 12053.
- (12) Savio, L.; Celasco, E.; Vattuone, L.; Rocca, M. *J. Phys. Chem. B* **2004**, *108*, 7771.
- (13) Altieri, S.; Contri, S. F.; Valeri, S. *Phys. Rev. B* **2007**, *76*, 205413.
- (14) Ferrari, A. M.; Roetti, C.; Pisani, C. *Phys. Chem. Chem. Phys.* **2007**, *9*, 2350.
- (15) Schintke, S.; Messerli, S.; Pivetta, M.; Patthey, F.; Libioule, L.; Stengel, M.; De Vita, A.; Schneider, W.-D. *Phys. Rev. Lett.* **2001**, *87*, 276801.
- (16) Sgroi, M.; Pisani, C.; Busso, M. *Thin Solid Films* **2001**, *400*, 64.
- (17) Peterka, D.; Tegenkamp, C.; Schröder, K.; Ernst, W.; Pfnür, H. *Surf. Sci.* **1999**, *431*, 146.
- (18) Wollschläger, J.; Viernow, J.; Tegenkamp, C.; Erdös, D.; Schröder, K. M.; Pfnür, H. *Appl. Surf. Sci.* **1999**, *142*, 129.
- (19) Kurth, M.; Graat, P. C. J.; Mittemeijer, R. J. *Thin Solid Films* **2006**, *500*, 61.
- (20) Campbell, C. T.; Valone, S. M. *J. Vac. Sci. Technol., A* **1985**, *3*, 408.
- (21) Kiguchi, M.; Goto, T.; Saiki, K.; Sasaki, T.; Iwasawa, Y.; Koma, A. *Surf. Sci.* **2002**, *512*, 97.

- (22) Valeri, S.; Altieri, S.; del Pennino, U.; di Bona, A.; Luches, P.; Rota, A. *Phys. Rev. B* **2002**, *65*, 245410.
- (23) Ferrari, A. M.; Casassa, S.; Pisani, C. *Phys. Rev. B* **2005**, *71*, 155404.
- (24) Wollschäger, J.; Erdös, D.; Schröder, K. M. *Surf. Sci.* **1998**, *402–404*, 272.
- (25) Scofield, J. H. *J. Electron Spectrosc.* **1976**, *8*, 129.
- (26) Ruffieux, P.; Schwaller, P.; Groning, O.; Schlalpbach, L.; Groning, P.; Herd, Q.C.; Funnemann, D.; Westermann, J. *Rev. Sci. Instrum.* **2000**, *71*, 3634.
- (27) Atieri, S.; Tjeng, L. H.; Voogt, F. C.; Hibma, T.; Sawatzky, G. A. *Phys. Rev. B* **1999**, *59*, R2517.
- (28) Corneille, J. S.; He, J.-W.; Goodman, D. W. *Surf. Sci.* **1994**, *306*, 269.
- (29) Huang, H. H.; Jiang, X.; Siew, H. L.; Chin, W. S.; Sim, W. S.; Xu, G. Q. *Surf. Sci.* **1999**, *436*, 167.
- (30) Schintke, S.; Schneider, W.-D. *J. Phys.: Condens. Matter* **2004**, *16*, R49.
- (31) Coustet, V.; Jupille, J. *Il Nuovo Cimento* **1997**, *19D*, 1657.